

# Account

## Mono and Multilayer Assembly of Zeolite Microcrystals on Substrates

Kyung Byung Yoon

*Center for Microcrystal Assembly, Department of Chemistry, and Program of Integrated Biotechnology,  
Sogang University, Seoul 121-742, Korea. E-mail: yoonkb@sogang.ac.kr*

*Received November 8, 2005*

We have shown that zeolite microcrystals can be readily organized in the form of uniformly oriented mono- and multilayers on various substrates by well-defined chemical linkages based on covalent, ionic, and hydrogen bondings between the microcrystals and the substrates. This finding establishes the fact that micrometer-scale building blocks can be readily organized into organized entities through interconnection of the surface-tethered large number of functional groups. Since zeolite crystals have highly regular and uniform nanochannels and nanopores within them, the resulting mono and multilayers of zeolite microcrystals bear great potential to be utilized in various novel applications.

**Key Words :** Zeolite, Microcrystal, Organization, Molecular linkers, Monolayer assembly

### Introduction

Assembly of small molecules in the form of thin films or organization of small molecules into highly ordered arrays of molecules on various supports has been the focus of interest during the last three decades as the ability to do so has many implications in materials science and in the development of new electronic and optoelectronic devices.<sup>1,2</sup> Scrutiny of the general trend of this area reveals that the sizes of building blocks (molecules) have gradually increased from relatively small molecules such as alkanethiolates<sup>3</sup> and octadecyltrichlorosilane<sup>4</sup> to much larger molecules such as enzymes (several nanometers)<sup>5</sup> and gold particles (several tens of nanometers).<sup>6,7</sup> Extrapolation of the above trend predicts that the sizes of building blocks will soon approach several hundred nanometers or even several micrometers. Under such circumstances, very large crystals or various systems of molecules will be encompassed into a class of building blocks. Indeed, it has been pointed out that 'modern chemistry is evolving away from the manipulation of sets of individual molecules toward the description and manipulation of systems of molecules.'<sup>8</sup> Therefore, the knowledge gained during the course of assembly of large building blocks, in particular, various micrometer-sized inorganic crystals by use of the surface-tethered nanometer-sized 'molecular linkers' or 'molecular binders', will help chemists

better understand nature's biomineralization processes and apply the acquired knowledge for the development of various advanced materials.

With the above background in mind, and by using zeolite crystals as the prototypical well-defined micro building blocks, we have demonstrated that the zeolite microcrystals can be indeed readily organized in the form of highly oriented mono- and multilayers on various substrates. This account summarizes the types of molecular linkages that have been developed in my group and the factors that govern the rate of monolayer assembly, the binding strength (BS) between each crystal and the substrate, and the degree of close packing.

### Results and Discussion

**Monolayer Assembly of Zeolite Microcrystals on Glass with Covalent Linkages.** As a test case, we first covalently tethered amino groups on the surfaces of zeolite-A crystals with the size of  $1 \times 1 \times 1 \mu\text{m}^3$  through n-propylsilyl groups using 3-aminopropyltriethoxysilane (AP-TES) as the reagent according to the scheme shown in Figure 1.<sup>9</sup> The fact that the surfaces of zeolite crystals are covered with hydroxyl groups was the basis for choosing the silylation as the methodology for tethering various functional groups including 3-aminopropyl (AP) groups. Independently, several

**Kyung Byung Yoon** received his B.S. from the Department of Chemistry, Seoul National University (1979). In 1981, he obtained his M.S. from the Department of Chemistry, Korea Advanced Institute of Science and Technology (KAIST), Seoul, where his research advisor was Professor Hakze Chon and his research field was hydrogenation reactions over metal-doped zeolites. From 1981 to 1984 he was employed by Chon Engineering Co. LTD, Seoul, Korea. In 1989, he earned his Ph.D. degree in inorganic chemistry from the Department of Chemistry, University of Houston, Houston, Texas, where his research advisor

was Professor Jay K. Kochi. He has been an Assistant, Associate (1993) and Professor (1998) at Sogang University from 1989 to the present. His research interest centers on the development of the methods of organizing zeolite microcrystals and applications of the resulting array of microcrystals. He was the Secretary General for the 11<sup>th</sup> Asian Chemical Congress which was held in Seoul, Korea in 2005. He served as a Vice-President of the Korean Chemical Society (2000, 2005), and is currently the Secretary General for the Federation of the Asian Chemical Societies.

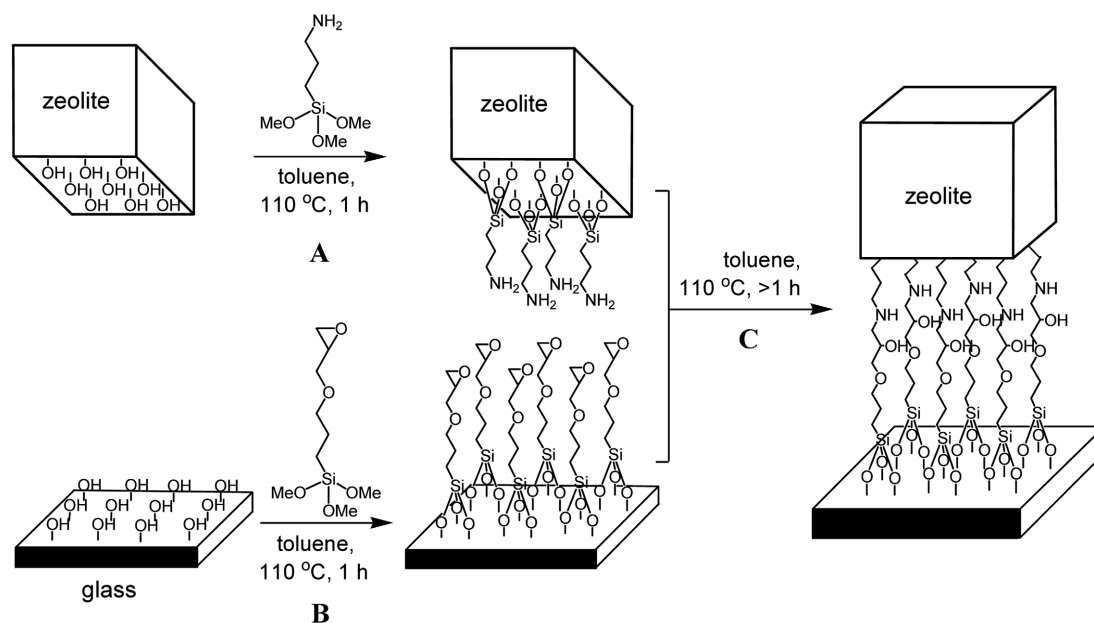


**Figure 1.** The schematic illustration of the procedure to attach zeolite-A crystals onto glass through surface-tethered AP and EP groups. Adopted from ref 9.

glass plates ( $18 \times 18 \text{ mm}^2$ ) tethering 3-(2,3-epoxypropoxy)propylsilyl groups on the surfaces were prepared using [3-(2,3-epoxypropoxy)propyl]trimethoxysilane (EP-TMS). Toluene has usually been the choice of the solvent for the surface modification of zeolites and glass and also for the subsequent attachment of zeolite crystals onto glass. When the toluene solution dispersed with AP-tethering zeolite-A crystals was refluxed for 3-24 h in the presence of EP-tethering glass plates which were mounted on a Teflon support, the zeolite-A crystals readily self-assembled in the form of monolayers on the glass substrates through formation of a large number of amine-alcohol linkages between the two solid surfaces as illustrated in Figure 1. The typical scanning electron microscopy (SEM) image of the monolayer is shown in Figure 2A. Visual observation of the zeolite-coated glass revealed that the entire glass plate was uniformly covered with zeolite-A crystals. Some physically adhered zeolite crystals were usually found on top of the zeolite-A monolayers. Luckily, they can be easily removed by weak sonication in toluene without detaching the first-layer zeolite crystals from the glass. However, care must be taken since even the covalently attached zeolite crystals can also fall off the glass if the sonication power was too high. Therefore, finding the appropriate sonication power is important for the preparation of zeolite-A monolayers free from physically adhered zeolite crystals.

Absence of one or both functional groups on the solid surfaces leads to the failure of the monolayer assembly. In such a case, only essentially empty glass plates that were only slightly coated with physisorbed zeolite crystals, which immediately fell off the glass plate even after sonication for 1 second, were obtained. This result unambiguously shows that the formation of amine-hydroxide linkage indeed readily undergoes between terminal amino and epoxy groups,

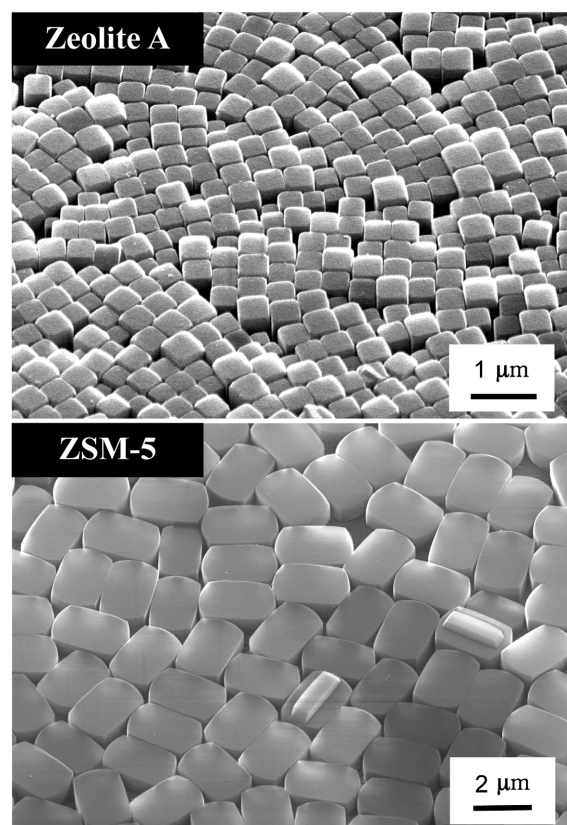


**Figure 2.** SEM images showing the closely packed, uniformly aligned monolayers of zeolite A (A) and silicalite (B) microcrystals assembled on glass.

leading to the effective monolayer assembly of zeolite-A crystals on the glass substrate.

The monolayers of the ZSM-5 crystals with the size of  $5 \mu\text{m}$  (along the *c*-axis) can also be readily assembled on glass

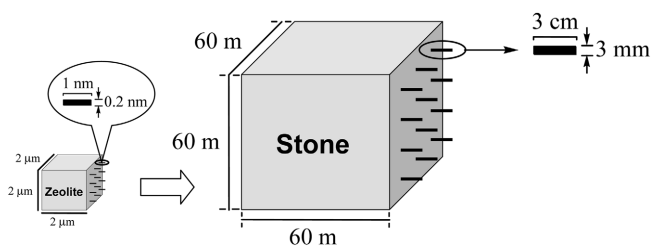


**Figure 3.** An illustration showing that the attachment of a zeolite-A crystal with the size of  $2 \times 2 \times 2 \mu\text{m}^3$  onto a glass substrate using the molecular linkers with the length of 1 nm and the thickness of 0.2 nm is equivalent to the attachment of a stone with the size of  $60 \times 60 \times 60 \text{ m}^3$  onto a conceptual wall using the strings with the length of 3 cm and the thickness of 6 mm.

plates using the same methodology, as shown in Figure 2B. The maximum size of the zeolite microcrystal that can be attached onto glass is  $\sim 10 \mu\text{m}$ . Above which, the zeolite crystals were too heavy to be attached onto glass using the above method. If a zeolite crystal with the size of  $2 \times 2 \times 2 \mu\text{m}^3$  was attached onto a glass plate through 1-nm long molecular linkers as is the above case, the situation can be compared to the attachment of a stone with the size of  $60 \times 60 \times 60 \text{ m}^3$  onto the wall using a large number of strings with the length of 3 cm and the thickness of 3 mm as illustrated in Figure 3.

Various other types of covalent linkages are shown in Figure 4. They are amine-fullerene-amine linkage (Figure 4A),<sup>10</sup> imine (-CH=N-) linkage that takes place between the formyl groups of terephthalaldehyde (TPDA) and the amino groups tethered to the surfaces of both zeolite and glass (Figure 4B),<sup>11</sup> secondary amine alcohol linkages that

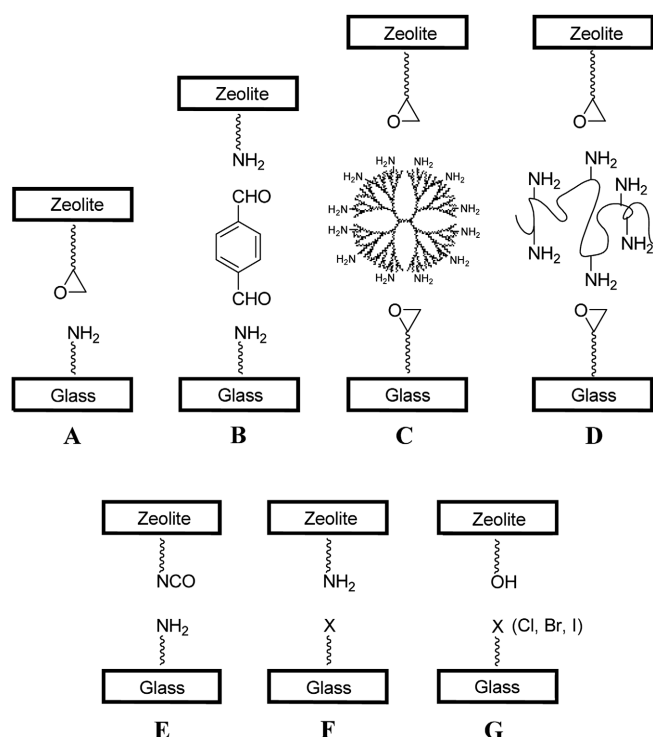


**Figure 4.** Various types of covalent molecular linkers.

are formed between the surface-tethered EP groups and dendritic polyamine (Figure 4C)<sup>12</sup> and polyethylene imine (Figure 4D),<sup>12</sup> respectively, urethane linkage (Figure 4E),<sup>13</sup> secondary amine linkage that is formed from the reaction between amino groups and 3-propyl halide (Figure 4F),<sup>14</sup> and the ether linkage that is formed by direct nucleophilic substitution of the halide ( $\text{Cl}^-$ ,  $\text{Br}^-$ , and  $\text{I}^-$ ) on the 3-halopropyl with the surface hydroxyl group of zeolite (Figure 4G).<sup>14</sup> The 3-halopropyl groups can also be tethered to the surfaces of zeolite crystals rather than to glass. However, from the practical point of view, it is more convenient to tether 3-halopropyl groups to glass plates. Among the above covalent linkages, the ether linkage formation (Figure 4G) is most useful from the practical point of view since it requires surface modification of only one solid, either glass or zeolite. Indeed this method has later been most widely used by our and other groups.

As well demonstrated in the SEM images shown in Figure 2, the zeolite microcrystals were attached onto glass plates with uniform orientations. For instance, each zeolite-A crystal was attached with a face parallel to the glass surface (Figure 2A). This is not unusual since all the three faces of a cubic zeolite-A are equivalent. Consistent with this, the x-ray diffraction pattern of the glass plate showed only (h 0 0) reflections ( $h = 2, 4, 6, 8, 10, \text{ and } 12$ ) as shown in Figure 5A. As noted, this diffraction pattern is very different from that

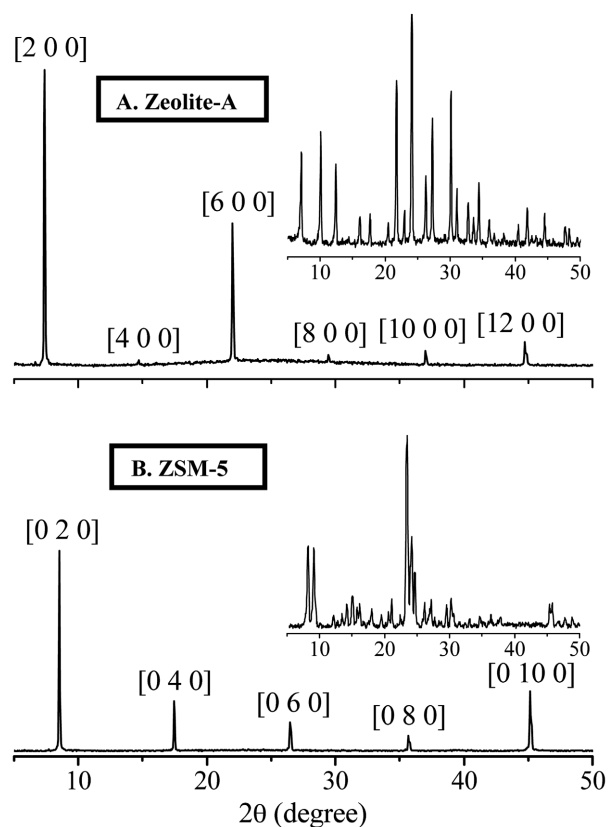


**Figure 5.** X-ray powder diffraction patterns of zeolite-A (A) and silicalite (B) monolayers assembled on glass showing the aligned state of crystals. Insets show the XRD patterns for randomly oriented powders of the zeolites. Adopted from ref 9.

of powder shown in the inset. This result also shows that the zeolite-A crystals are aligned in the same orientation over the entire glass plate.

The x-ray diffraction pattern of the glass plate attached with silicalite crystals showed only (0 k 0) reflection planes ( $k = 2, 4, 6, 8,$  and  $10$ ) as shown in Figure 5B, consistent with the SEM image shown in Figure 2B. This result shows that silicalite crystals align with the b-axes perpendicular to the plane of the glass plate on the entire glass plate. This diffraction pattern is also very different from that of powder shown in the inset. In fact, the (h 0 0) plane of the silicalite is also flat. Therefore, the silicalite crystals also have a chance to be attached onto glass with the a-axes perpendicular to the plane of the substrate. However, as shown in Figure 2B, it is difficult to find the silicalite crystals that are orienting with the a-axes perpendicular to the substrate plane. Thus, the zeolite microcrystals tend to attach onto glass plate through the largest-area face. In fact, as will be described later, the attached zeolite crystals are continuously replaced by those crystals that are dispersed in solution<sup>15</sup> Since the binding strength of the crystals will increase with increasing the contact area between each crystal and glass, the weakly attached crystals were more readily replaced by the zeolite crystals, allowing only most strongly attached crystals or the crystals attached with the largest-area face remain attached.

**Monolayer Assembly of Zeolite Microcrystals on Glass with Ionic Bonding.** The glass plates tethering trimethylpropylammonium iodide groups (denoted as  $G^+I^-$ ) and the zeolite (silicalite) crystals tethering sodium butyrate ( $Z^-Na^+$ ) were prepared (Figure 6A).<sup>16</sup> When the ethanol solution dispersed with  $Z^-Na^+$ s was shaken in the presence of  $G^+I^-$ s at 60 °C for 1 h, the  $Z^-$  crystals readily assembled in the form of closely packed monolayers on  $G^+$ . The same

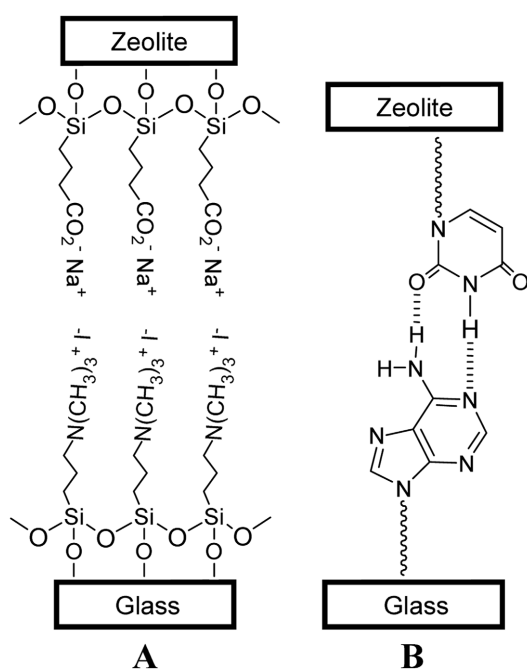


**Figure 6.** Molecular linkages based on ionic (A) and hydrogen (B) bonding.

methodology also worked well with the glass plates tethering sodium butyrate ( $G^-Na^+$ ) and the zeolite (silicalite) crystals tethering trimethylpropylammonium iodide groups ( $Z^+I^-$ ). The binding strengths of the zeolite crystals that were attached onto glass through ionic linkages were significantly higher than those of the zeolite crystals that were attached onto glass through covalent linkages. This occurs because the number of linkage that forms between each zeolite crystal and glass during the attachment reaction is higher with ionic linkage than with covalent linkage arising from the fact that ionic bonding is omnidirectional, works well regardless of the distance between the positive and negative centers although the bond strength is inversely dependent on the distance, and does not require the kinetic energies above a certain threshold unlike the covalent linkage which forms only when a functional group approach the other functional group with specific directions, angles, distances, and kinetic energies.

**Monolayer Assembly of Zeolite Microcrystals on Glass with Hydrogen Bonding.** Although H-bonding is much weaker than covalent and ionic bondings, we were able to show that it can also be used to assemble even the monolayers of 2.5- $\mu\text{m}$  sized zeolite microcrystals.<sup>17</sup> For this, we prepared silicalite crystals (size = 2.5  $\mu\text{m}$ ) and glass plates tethering thymine (T) and adenine (A), respectively, through an undecyl spacer (Figure 6B). For comparison, we also prepared silicalite crystals tethering 3-methylthymine (3-MT) groups. When the aqueous solution dispersed with T-tethering silicalite (T-SL) crystals was gently shaken for 3 h at room temperature in the presence of A-tethering glass plate (A-G), the T-SL crystals readily self-assembled in the form of closely packed monolayers on A-G. In contrast, the 3-methylthymine-tethering silicalite crystals did not form monolayers on A-G, demonstrating that A-T base pairing is essential for the monolayer assembly. The sonication-induced detachment test revealed that, as expected, the average binding strength between each zeolite crystal and glass surface is much weaker than those of the zeolite crystals attached to glass plates by the covalent and ionic linkages.

Interestingly, while it takes about 3 h to for the degree of coverage (DOC) to reach  $\sim 100\%$  between 25 and 50 °C, it takes only  $\sim 1$  h at 55 °C for the DOC to reach  $\sim 100\%$ , and

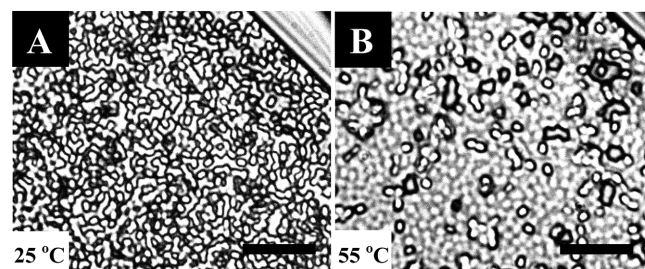


**Figure 7.** Optical microscope images of the randomly dispersed monolayer of thymine-tethering silicalite (T-SL) crystals on adenine-tethering glass (A-GL) obtained after 30 min at 25 °C (scale bar = 20  $\mu\text{m}$ ) (A) and a closely-packed monolayer of T-SL crystals after keeping the glass plate shown in (A) still in fresh water for 20 min at 55 °C. (B). Adopted from ref 17.



that with much higher degree of close packing (DCP). For instance, the optical microscope image of the A-GL which was allowed to contact with T-SL for 30 min at room temperature showed that the glass was covered mostly with small domains of closely packed crystals consisting of less than 10 crystals as typically shown in Figure 7A. However, the small domains underwent rapid merging into much larger closely packed domains (Figure 7B) when the glass plate was kept horizontal for 20 min in fresh water at 55 °C. Thus, the boundary between zeolite crystals becomes dim and fuzzy in the optical microscope image when the crystals closely pack. In contrast, such a phenomenon did not occur during such a short period of time at lower temperatures (< 50 °C). At higher temperatures (> 55 °C), the degree of close packing sharply decreased. This phenomenon occurs due to rapid bond breaking and bond reforming (annealing) between the surface-tethered complementary DNA bases at 55 °C, which allows facile migration of the crystals on the glass surface leading to close packing between the crystals. As for the driving force for the close packing, the weak hydrogen-bonding interaction between the surface-tethered T groups, hydrophobic interaction of the modified surfaces, and capillary forces are likely to be responsible.

**Effect of Agitation on the Rate of Monolayer Assembly.** Microcrystals are much heavier than small molecules and nanoparticles. Therefore, when they are dispersed in solutions, they have a strong tendency to precipitate at the bottom of the container when kept still. Reflux alone is usually not enough to fully disperse them into the solution. Therefore, constant stirring is necessary to keep them dispersed in the solution. Furthermore, it has been found that the kinetic energy gained by the microcrystal-tethered functional groups from the hot-refluxing solutions is usually not large enough for the functional groups to undergo linkage reaction with the functional groups tethered to substrates.<sup>15</sup> Therefore, the degree of agitation of the microcrystals is a very important factor that sensitively affects the reaction rate and the degree of close packing (DCP) of the crystals. To deduce above phenomenon, we tested three different modes of reaction employing 3-chloropropyl-tethering glass (CP-G) plates as the model substrates and bare zeolite crystals as the model zeolite microcrystals.<sup>15</sup>

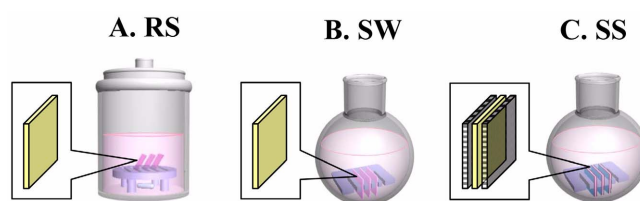


**Figure 8.** Experimental setups for reflux and stirring (RS), sonication without stacking (SW), and sonication with stacking (SS) of the CP-tethering glass plates (light) with bare glass plates (dark). Adopted from ref 15.

The first mode is reflux and stirring (RS) whose typical setup is shown in Figure 8A. The CP-G plates are placed on a Teflon support having four legs. A stirring bar is rotated under the support to stir the toluene solution of bare zeolite crystals while the reflux undergoes. The other two reaction modes were sonication without stacking (SW) and sonication with stacking (SS), respectively. The SW mode is to place CP-G plates as such without covering them with bare glass plates on both sides on a comb-like spacer that are placed at the bottom of a round-bottomed flask (Figure 8B). Sonication is carried out using a sonic bath. The SS mode is to make stacks of bare glass plate/CP-G/bare glass plate (BG/CP-G/BG) and then placing them on the comb-like spacer and subsequently sonicate them in a toluene solution dispersed with bare silicalite crystals (Figure 8C).

As shown in Figure 9A, it took ~3 h for the degree of coverage (DOC) to reach 90% under the RS condition. The DOC gradually increased to ~100% over the period of next 21 h. In strong contrast, however, it took only 1.5 min for the DOC to reach 100% when the reaction was carried out under the SW and SS conditions as compared in Figure 9B.

The SEM images of the CP-G plates which were allowed to react with bare silicalite for 10 min and 24 h, respectively, under the condition of RS are shown in Figure 10, A and B, respectively. The corresponding SEM images of the CP-G plates that were sonicated in the presence of bare silicalite crystals for 2 min under the SW and SS conditions, respectively, are shown in Figure 10, C and D, respectively. As noted, the DOC and the DCP of the silicalite monolayer that was formed under the SW condition for 2 min are compar-

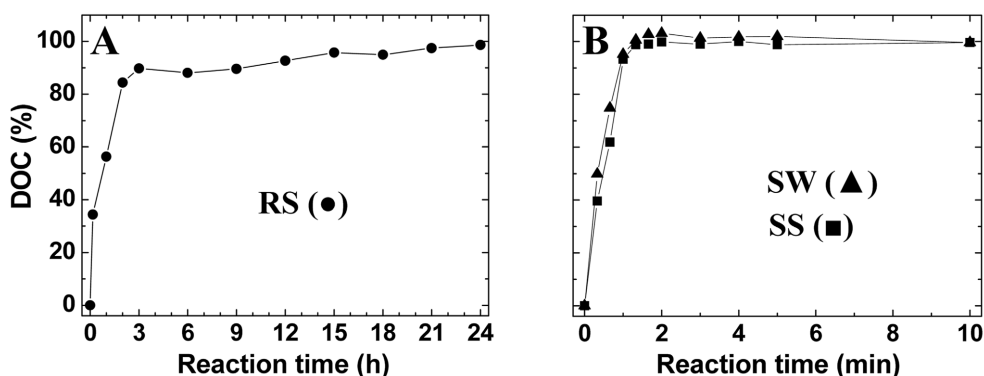


**Figure 9.** DOC-time profiles for the attachment of SL crystals onto CP-G during the period of shown in the x-axis, obtained under the conditions of RS (A) and SW and SS (B), respectively. Adopted from ref 15.

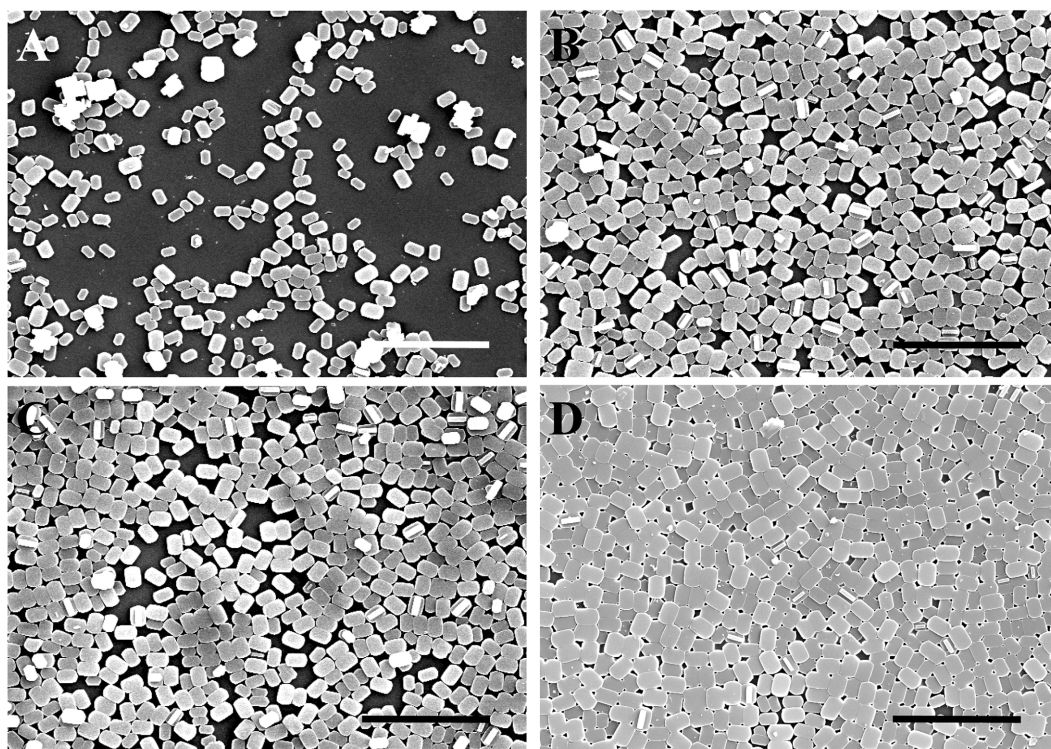


**Figure 10.** SEM images of SL monolayers assembled on CP-G plates by reacting the glass plates with bare SL crystals for 10 min (A) and 24 h (B) under the condition of RS and for 2 min under the conditions of SW (C) and SS (D), respectively. Adopted from ref 15.

able with those of the monolayer that was formed under the RS condition for 24 h. The DOC and DCP of the monolayer that was formed under the SS condition for 2 min were much higher than those of any other monolayers formed under other conditions.

As demonstrated above, the sonication-aided strong agitation of the zeolite microcrystals leads to a dramatic increase in the rate of monolayer assembly of the microcrystals on substrates due to the following phenomena. First, the strong agitation gives the microcrystals a large amount of translational energy which in turn gives the surface-tethered functional groups a large amount of translational energy to react with the substrate-tethered functional groups during collision. Second, the strong agitation facilitates the bond breaking and bond re-forming between the microcrystals and the substrates which is an essential element for the microcrystals to achieve close packing.

Interestingly, it was discovered that the microcrystals move from the bottom to the top between the glass plates when the reaction was carried out under the SS condition. The above phenomenon gives rise to the extraordinarily high DCP between the silicalite microcrystals observed from the monolayer that was obtained after sonication for 2 min under the SS condition (Figure 10D).

**Factors that Affect the Binding Strength. A. Use of Polymeric Linkers:** Unlike small molecules, a large number of interconnecting linkage is required for the microcrystals and the substrate to maintain adhesion with reasonable binding strength. Estimation shows that over 600,000 interconnecting linkages are possible between a face of a zeolite

microcrystal with the size of  $1 \times 1 \times 1 \mu\text{m}^3$  and the substrate provided that both surfaces are atomically flat.<sup>12</sup> However, the actual number of interconnecting linkage is expected to be much lower than the estimated number due to the unevenness of the surfaces of both zeolite and substrate in particular when the lengths of the surface-tethered molecular linkers are shorter than the peak-to-valley depths.

Since there are no established methods to measure the binding strengths between zeolite crystals and substrates we used sonication-induced detachment of the glass-bound zeolite crystals in clean toluene as a qualitative measure of the binding strengths. For this, we obtained the percentage of the remaining amount of zeolite crystals with respect to the initially fully attached amount (denoted as %R) after sonication of the glass plates in clean toluene for a desired period of time, and then plotted the %R with respect to sonication time. For each type of linkage, five samples were run separately, and the average remaining amount was plotted against sonication time.

Figure 11 shows three distinct profiles of %R with time obtained from three different glass-bound zeolite monolayers.<sup>12</sup> In the case of zeolite monolayers assembled by direct AP-EP linkage, %R reached to 20% after the initial 5-min sonication. In strong contrast, %R values were 83% and 93%, respectively, from the monolayers assembled with dendritic polyamine (DPA, generation 4 Starburst PAMAM dendrimer, with 64 surface primary amino groups) and polyethylenimine (PEI), respectively, as the linkers. After sonication for 1 h, the %R values reached 4%, 50%, and 75%, respectively, for AP-EP, EP-DPA-EP, and EP-PEI-EP

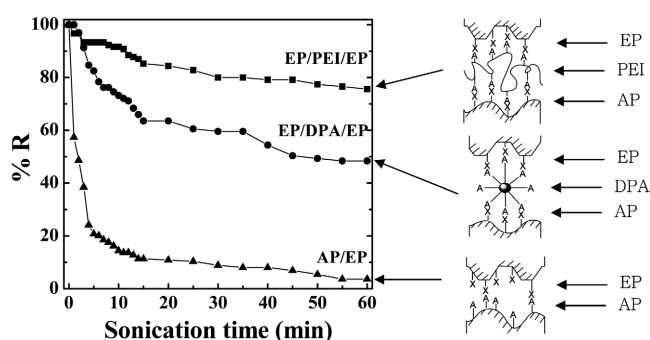


**Figure 11.** The plot of %R with respect to sonication time for the monolayers of EP-tethering zeolite-A crystals assembled on AP-tethering glass plate and on EP-tethering glass plates using DPA and PEI as the intermediate linkers, as indicated. Adopted from ref 12.

linkages, respectively. This result thus clearly establishes that the binding strength between zeolite crystals and the substrates increases dramatically by employing polyamines as the linkers. Such a result is attributed to the ability of the large polyamine linkers to position within the nanovalleys of the solid surfaces in such a way to increase the number of  $\beta$ -amino alcohol linkages between the multiple amine groups and the surface-tethered EP groups.

The aforementioned increase in binding strength upon changing the type of linkage from covalent to ionic bonding is also attributed to the net increase in the number of bonding due to the reasons described earlier. The qualitative comparison of the binding strength of the  $G^+Z^-$  with those of G-EP-AP-Z and G-EP-AP-Z is shown in Figure 12A. The binding strength between the ionically assembled monolayer of zeolite microcrystals and the substrate also significantly increased upon using polyelectrolyte such as poly(sodium 4-styrenesulfonate) ( $Na^+PSS^-$ ) and poly(diallyldimethylammonium chloride) ( $PDDA^+Cl^-$ ) as the linker, and with increasing the number of polyelectrolyte layer as shown in Figure 12B. The above comparison revealed that the binding strength between zeolite and glass in  $G^+PSS^-/PDDA^+/PSS^-/Z^+$  is stronger than that of  $G/EP/PEI/EP/Z$ . Accordingly, we used  $G^+PSS^-/PDDA^+/PSS^-/Z^+$  as the repeating unit for the multilayer (pentalayer) assembly of zeolite crystals on glass (Figure 13).

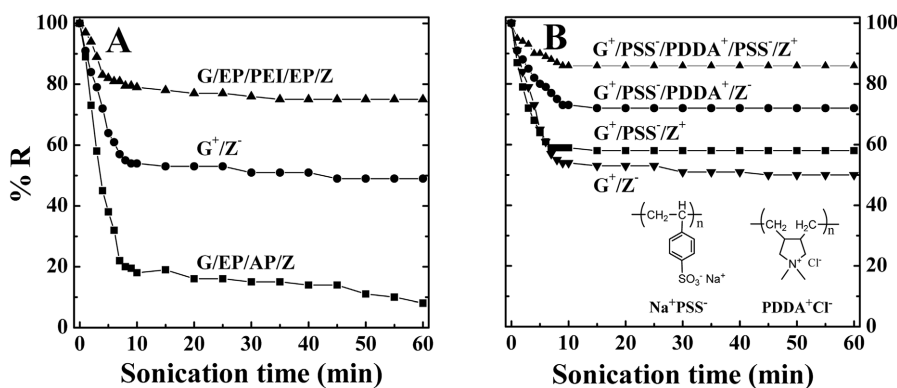


**Figure 12.** Comparison of the profile of %R with respect to the sonication time; the zeolite monolayers with three (A) and four (B) different types of linkage between zeolite crystals and glass plates (as indicated). Adopted from ref 16.

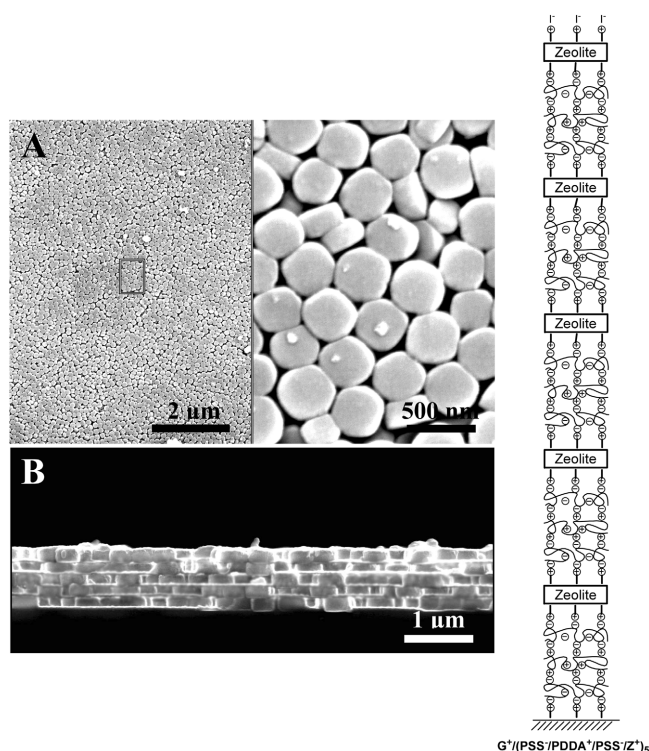


**Figure 13.** Typical SEM images of the outermost layer of  $G^+/PSS^-/PDDA^+/PSS^-/Z^+$ 5 at two different magnifications (A) and the corresponding cross section (B). Adopted from ref 16.

#### B. Cross-Linking between the Adjacent Microcrystals:

The lateral cross-linking between the neighboring, adjacent microcrystals also gives rise to a marked increase in the binding strength between the monolayers of zeolite microcrystals and the glass substrate despite the fact that the cross-linking did not increase the number of linkages between the microcrystals and the underlying glass substrate.<sup>18</sup> To demonstrate this, we prepared monolayers of AP-tethering cubic zeolite-A microcrystals ( $1.7 \times 1.7 \times 1.7 \mu m^3$ ) on the glass plates sequentially tethering AP and TPDA as shown in Figure 14A. Since each zeolite-A crystal has non-reacted AP groups on the other five faces, we further treated a monolayer of AP-tethering zeolite-A crystals with TPDA to cross-link the neighboring, closely contacting crystals

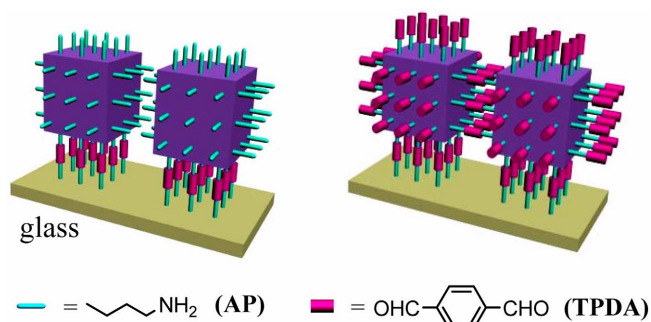


**Figure 14.** Illustration of the modes of linkages between the substrate and the zeolite microcrystals and between the closely packed neighboring microcrystals before (A) and after (B) cross-linking. Adopted from ref 18.

through AP-TPDA-AP linkages (Figure 14B).

The marked difference in the binding strength between the non-cross-linked and cross-linked monolayers of zeolite microcrystals is demonstrated in Figure 15. Thus, while more than 70% of non-cross-linked zeolite microcrystals fell off the glass plates after 30 min, that of the cross-linked zeolite microcrystals was less than 10%. This shows that the cross-linking leads to a 7-fold increase (by average) in binding strength between the monolayers and the substrates.

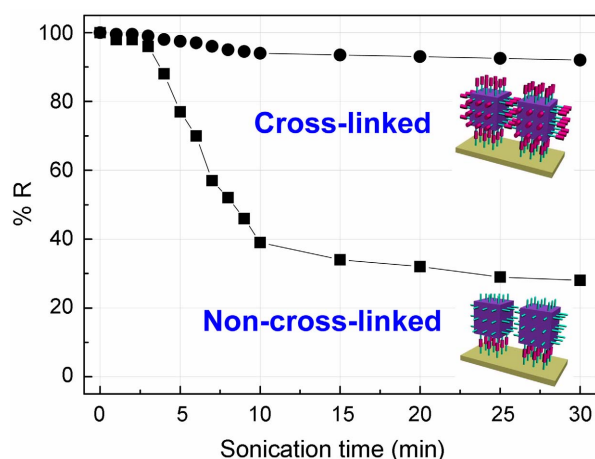


**Figure 15.** The plots of %R with respect to sonication time for the monolayers of AP-Z crystals assembled on glass plates with imine linkages before and after imine cross-linking between the neighboring crystals (as indicated). Adopted from ref 18.

Such a cross-linking-induced increase in the binding strength is more pronounced with decreasing the size of the crystals.<sup>18</sup> Indeed, it has been known that the cross-linking between the molecules self-assembled on substrates gives rise to a dramatic increase in the binding strengths between

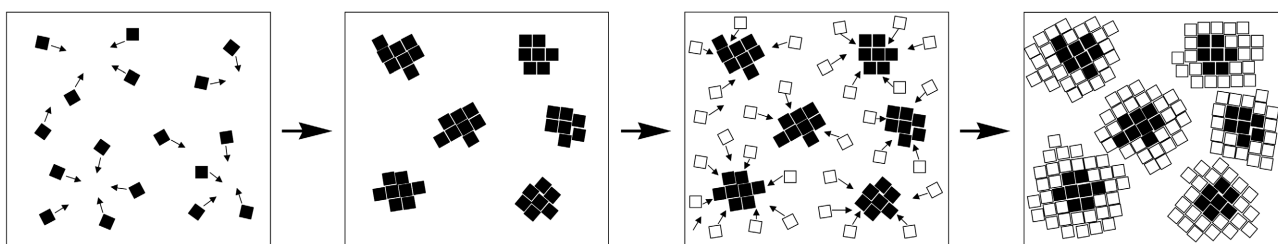


**Figure 16.** The surface migration mechanism for the phenomenon of close packing between crystals. Adopted from ref 10.

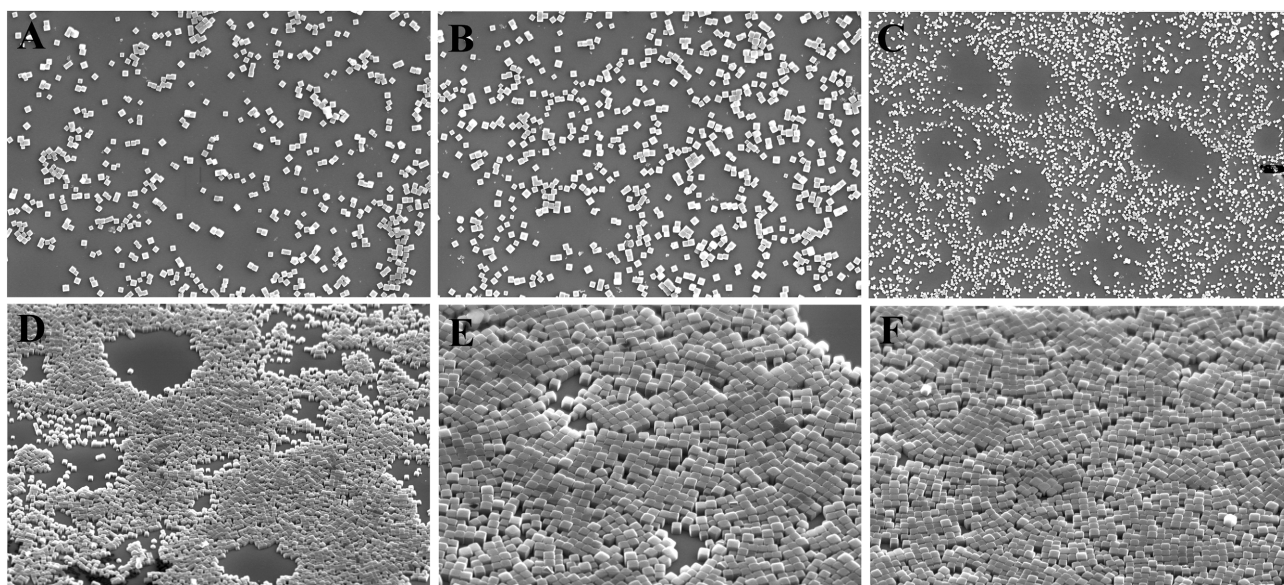


**Figure 17.** SEM images showing various spots with different degrees of coverage on a glass plate partially covered with zeolite-A crystals, at the magnifications of 3 K (A), 4 K (B), 1.5 K (C), 3 K (D), and 6 K (E, F). Adopted from ref 10.

the monolayers and the substrates.<sup>19,20</sup>

**C. Assembly with Strong Agitation:** We also found that the microcrystals were more strongly attached onto glass when the attachment reaction was carried out under the SS or SW condition.<sup>15</sup> For instance, the binding strength of the microcrystals attached to glass under the condition of SS for 1 h was 5.5 times stronger than that of the microcrystals that were attached to glass under the RS condition for the same period of time. This indicates that strong agitation leads to the increase in the number of bonding between the crystals and the substrates, due to stronger collision between the crystal and the substrate. However, it was also noted that the binding strength varies with time.

**Factors that Affect Close Packing.** As noted in Figure 2, the zeolite crystals tend to closely pack. It was revealed that the zeolite microcrystals move around on the surface during the assembly according to the scheme shown in Figure 16, and this phenomenon is responsible for the close packing between the microcrystals. During the monolayer assembly under the RS condition, the solvent bubbles generated from the surface of zeolite-attached substrate played an important role as shown in Figure 17. For the surface migration to occur, the cycle of bond-forming and bond-breaking should undergo. Therefore, there is a tendency for DCP to increase with decreasing the binding strength between the crystals and the substrate. For a given binding strength, the DCP increases with increasing the degree of agitation. Since the surface migration eventually leads to the decrease in the number of linkage, continued exposure of the zeolite-bound glass plates to reaction medium under the condition of high degree of agitation eventually leads to the loss of binding strength. This phenomenon was observed during the monolayer assembly of zeolite microcrystals under the condition of SW and SS.<sup>15</sup>

**Types of Substrates.** The types of substrates that have been tested so far are glass,<sup>9-18</sup> glass fiber,<sup>12</sup> silica,<sup>14</sup> alumina,<sup>14</sup> large zeolite,<sup>14</sup> vegetable fibers<sup>21</sup> such as cotton, linen, and hemp, artificial fibers<sup>22</sup> such as nylon, polyester, conducting substrates<sup>23</sup> such as Pt, Au, and ITO glass.

## Conclusion

Chemists have accumulated a great deal of knowledge to organize atoms and small molecules into small and large molecules, respectively, during the last century. Recently, a large number of chemists have also been interested in developing the methods of preparing uniform nanometer-sized particles and crystals and organizing them into functional entities. The atoms and small molecules can be regarded as the subnanometer-scale building blocks and the nanometer-sized particles and crystals as nanometer-scale building blocks. What we have pursued during the last several years is to develop the methods of organizing microcrystals, that is, micro building blocks into organized entities. As a possible means, we have developed the methods of organizing microcrystals into monolayers and multilayers in uniform orientation, using micrometer-scale zeolite crystals

as the model micro building blocks. We have demonstrated that microcrystals can also be readily organized into functional entities by tethering functional groups on their surfaces and subsequently interconnecting them through appropriate chemical reactions. In other words, we have shown that 'the chemistry of microcrystals is doable'. The thermal energy is not enough to give microcrystals enough kinetic energy. Therefore, under the condition of reflux and stirring, which has been the routine source of kinetic energy for small molecules to undergo reaction, the surface-tethered functional groups do not readily undergo interconnecting reactions. So, strong agitation is essential for the microcrystal-tethered functional groups to undergo the desired interconnecting reactions. We believe our finding will provide chemists and materials scientists with the opportunity to diversify their repertoires of building blocks from subnanometer to micrometer scales. The micro-patterned monolayer assembly<sup>24,25</sup> and the direct orientation-controlled monolayer assembly during the synthesis of zeolite crystals,<sup>26</sup> which are not covered in this Account, will further diversify the microcrystal chemistry we have developed. The resulting zeolite mono and multilayers also bear great potential to be utilized for the characterization of paramagnetic species existing within zeolites,<sup>27</sup> as high quality molecular sieving membranes<sup>28</sup> and advanced materials.

**Acknowledgements.** I thank the graduate students and the postdoctoral research fellows whose name appear in the references for their hard work which made this Account possible. I also thank the Ministry of Science and Technology (MOST), and Sogang University for supporting this work through the Creative Research Initiatives (CRI), and the Internal Research Fund programs, respectively.

## References

1. Petty, M. C. *Langmuir-Blodgett Films an Introduction*; Cambridge University Press: Cambridge, UK, 1996.
2. (a) *Characterization of Organic Thin Films*; Ulman, A.; Fitzpatrick, L. E., Eds.; Butterworth-Heinemann: Boston, MA, 1995. (b) Ulman, A. *An Introduction to Ultrathin Organic Films*; Academic Press: Boston, 1991. (c) Ulman, A. *Chem. Rev.* **1996**, *96*, 1533.
3. Nuzzo, R. G.; Allara, D. L. *J. Am. Chem. Soc.* **1983**, *105*, 4481.
4. Sagiv, J. *J. Am. Chem. Soc.* **1980**, *102*, 92.
5. Riklin, A.; Willner, I. *Anal. Chem.* **1995**, *67*, 4118.
6. (a) Lyon, L. A.; Rena, D. J.; Natan, M. J. *J. Phys. Chem. B* **1999**, *103*, 5826. (b) Grabar, K. C.; Freeman, R. G.; Hommer, M. B.; Natan, M. J. *Anal. Chem.* **1995**, *67*, 735.
7. (a) Brust, M.; Kiely, C. J.; Bethell, D.; Schiffrin, D. J. *J. Am. Chem. Soc.* **1998**, *120*, 12367. (b) Brust, M.; Bethell, D.; Kiely, C. J.; Schiffrin, D. J. *Langmuir* **1998**, *5*, 5425.
8. Whitesides, G. M.; Ismagilov, R. F. *Science* **1999**, *284*, 89.
9. Kulak, A.; Lee, Y. J.; Park, Y. S.; Yoon, K. B. *Angew. Chem. Int. Ed.* **2000**, *39*, 950.
10. Choi, S. Y.; Lee, Y.-J.; Park, Y. S.; Ha, K.; Yoon, K. B. *J. Am. Chem. Soc.* **2000**, *122*, 5201.
11. Lee, G. S.; Lee, Y.-J.; Ha, K.; Yoon, K. B. *Tetrahedron* **2000**, *56*, 6965.
12. Kulak, A.; Park, Y. S.; Lee, Y.-J.; Chun, Y. S.; Ha, K.; Yoon, K. B. *J. Am. Chem. Soc.* **2000**, *122*, 9308.
13. Chun, Y. S.; Ha, K.; Lee, Y.-J.; Lee, J. S.; Kim, H. S.; Park, Y. S.;

- Yoon, K. B. *Chem. Commun.* **2002**, 1846.
14. Ha, K.; Lee, Y.-J.; Lee, H. J.; Yoon, K. B. *Adv. Mater.* **2000**, *12*, 1114.
15. Lee, J. S.; Ha, K.; Lee, Y.-J.; Yoon, K. B. *Adv. Mater.* **2005**, *17*, 837.
16. Lee, G. S.; Lee, Y.-J.; Yoon, K. B. *J. Am. Chem. Soc.* **2001**, *123*, 9769.
17. Park, J. S.; Lee, G. S.; Lee, Y.-J.; Park, Y. S.; Yoon, K. B. *J. Am. Chem. Soc.* **2002**, *124*, 13366.
18. Park, J. S.; Lee, Y.-J.; Yoon, K. B. *J. Am. Chem. Soc.* **2004**, *126*, 1934.
19. (a) Kim, T.; Chan, K. C.; Crooks, R. M. *J. Am. Chem. Soc.* **1997**, *119*, 189. (b) Chan, K. C.; Kim, T.; Schoer, J. K.; Crooks, R. M. *J. Am. Chem. Soc.* **1995**, *117*, 5875. (c) Lackowski, W. M.; Ghosh, P.; Crooks, R. M. *J. Am. Chem. Soc.* **1999**, *121*, 1419. (d) Huck, W. T. S.; Yan, L.; Stroock, A.; Haag, R.; Whitesides, G. M. *Langmuir* **1999**, *15*, 6862. (e) Husemann, M.; Mecerreyes, D.; Hawker, C. J.; Hedrick, J. L.; Shah, R.; Abbott, N. L. *Angew. Chem., Int. Ed.* **1999**, *38*, 647.
20. It has also been repeatedly demonstrated that even the weak van der Waals interactions between the closely packed alkylmercaptan molecules selfassembled on gold surfaces significantly contribute to the stability of selfassembled monolayers. See: (a) Ulman, A. In *Thin Films; Self-Assembled Monolayers of Thiols*, Vol. 24; Academic Press: San Diego, 1998; pp 112-114. (b) Ulman, A. *Chem. Rev.* **1996**, *96*, 1533.
21. Lee, G. S.; Lee, Y.-J.; Ha, K.; Yoon, K. B. *Adv. Mater.* **2001**, *13*, 1491.
22. Lee, J. S.; Yoon, K. B., unpublished result.
23. Ha, K.; Park, J. S.; Oh, K. S.; Zhou, Y. S.; Chun, Y. S.; Lee, Y.-J.; Yoon, K. B. *Micropor. Mesopor. Mater.* **2004**, *72*, 91.
24. Ha, K.; Lee, Y.-J.; Jung, D.-Y.; Lee, J. H.; Yoon, K. B. *Adv. Mater.* **2000**, *12*, 1614.
25. Ha, K.; Lee, Y.-J.; Chun, Y. S.; Park, Y. S.; Lee, G. S.; Yoon, K. B. *Adv. Mater.* **2001**, *13*, 594.
26. Lee, J. S.; Lee, Y.-J.; Tae, E. L.; Park, Y. S.; Yoon, K. B. *Science* **2003**, *301*, 818.
27. So, H.; Ha, K.; Lee, Y.-J.; Yoon, K. B.; Belford, R. L. *J. Phys. Chem. B* **2003**, *107*, 8281.
28. Lai, Z.; Bonilla, G.; Diaz, I.; Nery, J. G.; Sujaoti, K.; Amat, M. A.; Kokkoli, E.; Terasaki, O.; Thompson, R. W.; Tsapatsis, M.; Vlachos, D. G. *Science* **2003**, *300*, 456.
-